IOSR Journal of Dental and Medical Sciences (IOSR-JDMS)
e-ISSN: 2279-0853, p-ISSN: 2279-0861.Volume 13, Issue 5 Ver. IV. (May. 2014), PP 50-61
www.iosrjournals.org

Protective role of coenzyme Q $_{10}$ against high cholesterol diet-induced histological and biochemical changes in cerebellar cortex of adult albino rats

Manal R. Abd El-Haleem[1], Ossama I. Yassen[1] and Nermin Raafat[2]
[1]*Histology Department, Faculty of Medicine, Zagazig University, Egypt.*
[2]*Medical Biochemistry Departement, Faculty of Medicine, Zagazig University, Egypt.*

Abstract: *Hypercholesterolemia was known to cause cardiovascular and brain damaging effects; however cholesterol is less known for affecting cerebellar and microvasculature pathology. Coenzyme Q_{10} (CoQ_{10}) is a naturally occurring potent antioxidant. The aim of this research is to study histological and biochemical alterations occuring in the structure of cerebellum after feeding high cholesterol diet and the possible protective role of CoQ_{10}. Forty male adult albino rats were randomly divided into four groups. Group I, control received a low-cholesterol diet. Group II received normal laboratory diet and CoQ_{10}, Group III fed on 5% cholesterol diet. Group IV fed on 5% cholesterol diet and CoQ_{10} orally. After 4 months the body weight of all rats was measured and lipid profile was assessed. Rats' cerebelli were removed, cortices were dissected and divided into three parts for histological, tau and GFAB immunohistochemical study and for assessment of endogenous oxidative and antioxidant markers. In cerebellar cortex from rats fed on high cholesterol diet, Purkinje cell number showed significant decrease compared to control group. They had many multi-lysosomes, cytoplasmic vacuoles, dilatation of rough endoplasmic reticulum and most of their nuclei were variable in shape, muddy or appoptotic, while few were euchromatic. In group IV, cerebellar cortex nearly regained the normal architecture but few granular cells still had pyknotic nuclei and few purkinje cells still had positive Tau immune reaction. High cholesterol diet has a deleterious effect on histological and biochemical structure of the cerebellum. Coenzyme-Q_{10} ameliorates these effects.*

Keywords: *high cholesterol diet, cerebellum, oxidative stress, Coenzyme Q_{10}.*

I. Introduction

Although the cerebellum constitutes only 10% of the total brain weight, it contains more than half of all the neurons in the brain. The cerebellum is responsible of coordination of voluntary movement, gait, posture, speech, and motor functions [1]. It also have a role in behavior, cognition, psychiatric illness, motor planning as well as discrimination of sensory information [2].

Cholesterol is an essential component of cell membrane and it is essential in many biochemical processes and support building cell membranes [3], but hypercholesterolemia is proved to be associated with negative health outcomes as cardiovascular diseases[4].

Almost all of the cholesterol in the brain is synthesized in the brain and little or none of the peripheral cholesterol crosses the blood– brain barrier. Thus it has been unclear to what extent dietary cholesterol can produce increases in brain cholesterol [5]. However, clinical observations strongly suggested the presence of exchange between brain and plasma compartments [6]. On the other hand, circulating cholesterol is bound up in lipoproteins low-density lipoprotein (LDL) and high-density lipoprotein (HDL), which enter cells by transcytosis at LDL receptors [7].

There are some controversy regarding the effect of a high cholesterol diet on the central nervous system. Some researchers recorded increase memory retention in rabbits fed high cholesterol diet [8]. It is associated with a lower risk of Parkinson's disease [9]. Microvessels and blood-brain barrier disruptions induced by elevated cholesterol both in vivo and in vitro which was associated with an increased risk of Alzheimer disease (AD) pathogenesis [6].

Non-pharmacological measures like dietary restriction and exercise failed to lower blood cholesterol levels in many cases of hypercholesterolaemia. Though, drug therapy like statins, fibrates and nicotinic acid are very effective, they have a spectrum of adverse effects [10].

Glial fibrillary acidic protein (GFAP) is considered a marker protein for severe activation of astrocytes (astrogliosis). Astrocytes are the major glial cell population within the CNS. They play important roles in CNS homeostasis through the release of several neurotrophic factors. Tau is a phosphoprotein that promotes tubulin polymerization and stabilizes microtubule structure in vivo. This function is crucial for the integrity of the neuronal cytoskeletal networks and the neuronal processes in forming connections with other cells [11].

However Tau is minimally phosphorylated in the normal adult brain. It is hyperphosphorylated in several neuro-degenerative conditions, including AD [12].

Coenzyme-Q_{10} (2,3dimethoxy-5methyl-6-decarpenyl benzoquinone) is a fat-soluble, vitamin-like quinine commonly known as ubiquinone. It is capable of influencing cellular bioenergetics and counteracting some of the damage caused by free radicals [13]. Co Q10 showed effectiveness in the treatment of some neurodegenerative disease. SO, the aim of this work was to elucidate the histological changes that might occur in the structure of the cerebellar cortex after feeding on high cholesterol diet and the possible protective role of Co Q_{10} [14].

II. Materials & Methods

Forty healthy male albino rat 12 weeks old, weighting 200–250 g were used in this study. Rats were purchased from the Animal House of the Faculty of Veterinary Medicine, Zagazig University, Egypt. They were housed in a stainless steel cages and maintained in room temperature at a 12-h light-dark cycle. All procedures in this study were performed in accordance with the medical research ethics committee of Zagazig University. All rats were acclimatized to the laboratory environment for 8 days before the start of the experiment.

2.1. Experimental design

Rats were randomly divided equally into four groups. Group I (control) received a standard low-cholesterol rodent chow diet containing 0.02% cholesterol and 6% fat (Lab Diet 5K52; Purina, St. Louis, MO). Group II (Q) received normal laboratory chow diet and co enzyme Q_{10}, Group III (HC) fed on 5% cholesterol diet (Harlan Teklad Co. Madison, WI, USA). Group IV (HC- Q_{10}) fed on 5% cholesterol diet and concomitantly received Co enzyme- Q $_{10}$ by oral gavage in a dose of 1mg /rat (Mepaco company). All rats were fed their respective diets and had access to water ad libitum for periods of 4 months .

The body weight of the experimental animals was measured at the start of the experiment (starting body weight), and after 4 months using a digital balance. The weight was usually determined at a fixed time in the morning. At the end of the experiment, all rats were fasted for 10h, but water was not restricted.

2.2. Sampling

Blood samples were taken for assessment of lipid profile including triglycerides, total cholesterol, HDL-C, and LDL-C. The animals were sacrificed by transcardial perfusion with cold 1% paraformaldehyde in 0.1 M PBS pH 7.4 (phosphate buffered saline) for 1 min, followed by cold 4% paraformaldehyde in 0.1 M PBS pH 7.4 for 10 min [15]. The skulls were carefully opened. Rats cerebelli were removed, cerebellar cortices were dissected out and divided into three parts. The first part for histological study, postfixed in 10% buffered formalin. The second part postfixed in 2.5% phosphate-buffered glutaraldehyde for ultrastructural study. The third part put in liquid nitrogen for tissue biochemical study for assessment of tissue endogenous antioxidant markers and oxidative markers.

2.3. Histological study

Specimens for light microscope examination were fixed in 10 % buffered formol saline for 24 hours and were processed to prepare 5 μm thick paraffin sections for haematoxylin and eosin stains and immunohistochemical study.

2.4. Immunohistochemical study

The immunohistochemical staining for localization of the GFAB and Tau protein was carried out by means of the avidin biotin– peroxidase complex method following the manufacturer’s instructions (Dako company, Wiesentheid/Bavaria, Germany, Biotin Blocking System, Code X0590). Paraffin sections of 4μm were deparaffinized in xylene and rehydrated in a descending series of ethanol. The specimens were subjected to antigen retrieval in a citrate buffered solution (pH 6.0) for 10 min using a microwave. Endogenous peroxidase was eliminated by incubation in 10% H_2O_2 in phosphate-buffered saline (PBS), pH 7.4 for 10 min. After washing, the specimens, were blocked in ready-use normal goat serum for 20min at room temperature. Then, the sections were incubated with the specific primary antibody at room temperature (Lab Vision Corporation, Medico Co. Egypt).

The primary antibody specific for GFAP in astrocytes used was a mouse monoclonal antibody Ab-1 (Clone GA-5), (Cat. #MS-280-B0), at 1:100 dilution for 20 min and for hyperphosphorylated tau, MAP 2a,b,c (Microtubule-Associated Protein) Ab-3 (Clone AP18), (Cat. MS-250-R7) at 1:5000 dilution for 30 minutes. Dilutions were done with antibody diluent (TA-125-UD; Lab Vision) .

Peroxidase activity was demonstrated using an AEC (3-amino-9-ethyl carbazole) substrate kit (TA-004-HAC; Labvision). The sections were rinsed in PBS. It was applied overnight (1:200) in a humidified chamber at 4˚C then washed in PBS twice. The secondary antibody was anti-rabbit antibody universal kit (code no. Ko773, lot). Sections were covered with biotinylated secondary antibody for 30 min and then washed in PBS. Then by peroxidase–labeled avidin/ biotin solution reaction (NovoStain Super ABC Kit, Novocastra, Newcastleupon –Tyne, UK) for 45 min. then washed in PBS. Finally, freshly prepared diaminobenzidine (Sigma, St. Louis, MO) was added for 4 min. A chromogen, washed with distilled water followed by Mayer's haematoxylin as a counter stain. The sections were washed, dehydrated mounted and examined. For the negative control, the same steps were followed, but the primary antibody was replaced by PBS[16].

2.5. Electron microscope study

Specimens for electron microscopy study were immediately fixed in 2.5% phosphate-buffered glutaraldehyde (pH 7.4). Then, they were postfixed in 1% osmium tetroxide in the same buffer at 4°C, dehydrated, and embedded in epoxy resin [17]. Semithin sections (1μm thick) were stained with 1% toluidine blue for light microscopic examination [18]. Ultrathin sections were stained with uranyl acetate and lead citrate [17] and examined and photographed using a JEOL JEM 1010 electron microscope (JEOL, LTD, Tokyo, Japan) in the Electron Microscope Research Laboratory of the Histology and Cell Biology Department, Faculty of Medicine, Zagazig University, and in the JEOL JEM 1200 EXII Electron Microscope (JEOL, LTD) Research Laboratory, Faculty of Science, Ain Shams University (Egypt).

2.6. Morphometrical study

The image analyzer computer system; Leica Qwin 500 (Leica LTD, Cambridge, UK) in the Image Analyzing Unit of the Pathology Department, Faculty of Dentistry, Cairo University (Egypt), was used to evaluate the following parameters in all studied groups:

1. Estimation of the thickness of the granular and molecular layers.
2. Linear density of Purkinje cells was determined by counting Purkinje cells nuclei per millimeter line length throughout the section [19].
3. The area percentage of the positive immune reaction for GFAP and Tau in the cerebellar cortex using immunostained sections were seen and were then masked by blue binary color to be measured. It was measured using the interactive measure menu to detect it in a standard measuring frame of a standard area equal to 118 476.6 mm^2.

All of the above parameters were measured by total magnification ×400 using 10 readings from 5 non-overlapped sections from each rat of the randomly chosen 5 rats in each group.

Blood samples were collected from orbital venous plexus in plain tubes, centrifuged at 2000 rpm for 20 min and blood sera were then collected and stored at 4°C prior immediate determination of triglycerides [20], total cholesterol, HDL-cholesterol and LDL-cholesterol [21]. All of these parameters were measured using spectrophotometer .

2.7. Tissue biochemical study

The cortices of the cerebelli were excised, wrapped with aluminum foil and immediately embedded in liquid nitrogen for freezing at −70°C for 1 h. Frozen tissue from each rat was homogenized in ice-cold phosphate buffer (KCl 140 mmol/l, phosphate 20 mmol/l, pH 7.4) and centrifuged at 3000 rpm for 10 min. The supernatant was used for the measurement of tissue superoxide dismutase (SOD) [22], catalase (CAT) [23] and endogenous glutathione peroxidase (GPx) [24], as antioxidant markers. The SOD, CAT and GPx, were determined using commercial kits (Bio Diagnostic company, Dokki, Giza, Egypt) with the catalogue number 2520, 2516 and 2524, respectively. Meanwhile, the concentration of malodialdehyde (MDA) was measured as an index of lipid peroxidation and oxidative stress [25].

2.8. Statistical analysis

Data for all groups were expressed as mean±SD (X±SD). The data obtained from the image analyzer and the biochemical data were subjected to SPSS program version 14 (http://www.spss.com, Chicago, Illinois, USA). Statistical analysis using the one-way analysis of variance test (ANOVA) was carried out to determine differences between the mean values of experimental groups. The t-test was used to compare control group with other groups. Post hoc test was used to find the statistical difference between groups. The results were considered statistically significant when P values were 0.001.

III. Results

The final body weight after 8 weeks was 375–400 g in the control group and 460–500 g in the HC group.

3.1. Histopathological results

3.1.1. Light microscope results

Light microscope of H&E-stained sections and toluidine blue stained semithin sections of both control group and group Q showed similar structure. So, Figures for group I were used with other groups. Light microscope of H & E-stained sections and toluidine blue stained semithin sections from control group revealed that the cerebellar cortex was formed of three layers: the outer molecular layer, the middle Purkinje cell layer, and the inner granular layer. The molecular layer had few small scattered cells. Purkinje cells, were pyriform in shape and arranged in one row. They had large round, vesicular nuclei with prominent nucleoli. The Purkinje cells were surrounded by few Bergman's astrocytes. The granular layer was formed of numerous crowded small granular cells with rounded pale nuclei (Fig. 1A&1D). Examination of H&E stained sections and toluidine blue stained semithin sections from HC group revealed that most of the Purkinje cells had deeply stained cytoplasm and pyknotic, ill-defined nuclei. Most of cells of granular cells had pale nuclei with peripheral clumps of heterochromatin while some granular cells had clumping deeply stained nuclei (Fig. 1B &1E). Examination of H&E-stained sections and toluidine blue stained semithin sections from HC– Q 10 group revealed that Purkinje cells had almost normal appearance. They had pyriform shape and pale vesicular nuclei with prominent nucleoli. Many swollen Bergmann cells are seen. Granular cell layer had pale nuclei (Fig. 1C & 1 F).

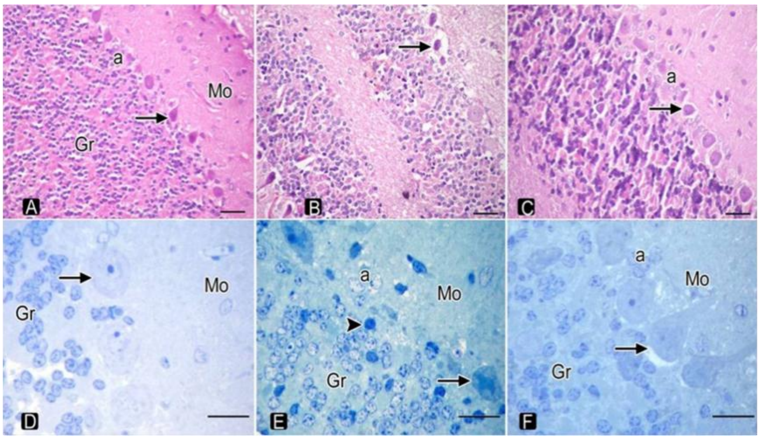

Fig. 1 A, B, C are H&E stained sections of cerebellar cortex of albine rat of all studied groups. **A:** control group shows small scattered cells of the molecular layer (Mo), single row of large pyriform shaped cells (arrows) of Purkinje cell layer, some Bergman astrocytes (a) and granular cell layer (Gr) with numerous crowded granular cells. **B:** HC group shows deeply stained Purkinje cells with ill-defined nuclei (arrows). **C:** HC– Q 10 group shows Purkinje cells (arrows) with pale vesicular nuclei arranged in single row and Bergmans astrocytes (a). D, E, F are toluidin blue stained semithin sections of cerebellar cortex of albino rat of all studied groups. **D:** control group shows pyriform Purkinje cell (arrows) with large rounded vesicular nucleus wit prominent nucleolus. Granular cells (Gr) have rounded pale nuclei and molecular layer (Mo) are seen. **E:** HC group shows Purkinje cells (arrows) with darkly stained cytoplasm and pyknotic, hardly identified nuclei. Bergmann astrocytes (a) are seen. Most of cells of granular cells (Gr) have pale nuclei with peripheral clumps of heterochromatin while some granular cells have clumping deeply stained nuclei (arrow heads). **F:** HC– Q 10 group shows Purkinje cells (arrows) have pyriform shape and pale vesicular nuclei with prominent nucleoli and many swollen Bergmann cells are seen (a). Granular cell layer (Gr) have pale nuclei. (Scale bar=50μm).

Immunohistochemically stained sections for GFAP of the control group showed scattered GFAP positive cells in the molecular and granular layers (Fig. 2A). HC group showed increase abundant large GFAP positive cells mainly in the molecular layer and granular layer (Fig. 2B). HC- Q10 group showed, few GFAP positive cells in the molecular and granular layers (Fig. 2C).

Immunohistochemically stained sections for the Tau protein, of the control group showed a negative immunoreaction in the three layers (Fig. 2D). HC group showed Tau positive reaction in most of Purkinje cells (Fig. 2E). HC – Q 10 group showed; few Tau positive reaction in the Purkinje cells. (Fig. 2E).

3.1.2. Electron microscopic results

Electron microscope examination of molecular layer of cerbellar cortex of control rats showed that, almost all nerve fibers are surrounded by normal myelin sheath (Fig. 3A). HC group showed that the myelin sheath showed focal areas of myelin sheath separation (Fig. 3B). HC–Q 10 group showed normal myelin sheath (Fig. 3C). Nerve cells of the molecular layer from cerebellar cortex of albine rat of all studied groups had euchromatic nuclei (Fig. 3A-C). Examination of the control group revealed that Purkinje cells had euchromatic nuclei and prominent nucleoli. Their cytoplasm was rich in organelles as strands of rough endoplasmic reticulum reticulum, small electron dense mitochondria, free ribosomes (Fig. 3D). Examination of the HC- group revealed atrophic changes in Purkinje cells. Some cells were shrinked leaving empty spaces around them (Fig. 3E). Purkinje cell with ill- defined muddy nucleus and marked indentation of the nuclear membrane and their cytoplasm had dilated rough endoplasmic reticulum (Fig. 3F). Their cytoplasm of Purkinje cell containing multiple lysosomes (Figs. 3E-G). Few Purkinje cells had euchromatic nuclei and well-defined nucleoli and their cytoplasm contained dilated perinuclear and rough endoplasmic reticulum cisternae (Fig. 3H). Examination of Purkinje cell of HC- Q 10 showed that they had euchromatic nuclei with deep indentation in the nuclear envelop. Their cytoplasm was rich in organells as mitochondria, ribosomes and short strands of rough endoplasmic reticulum (Fig.3I).

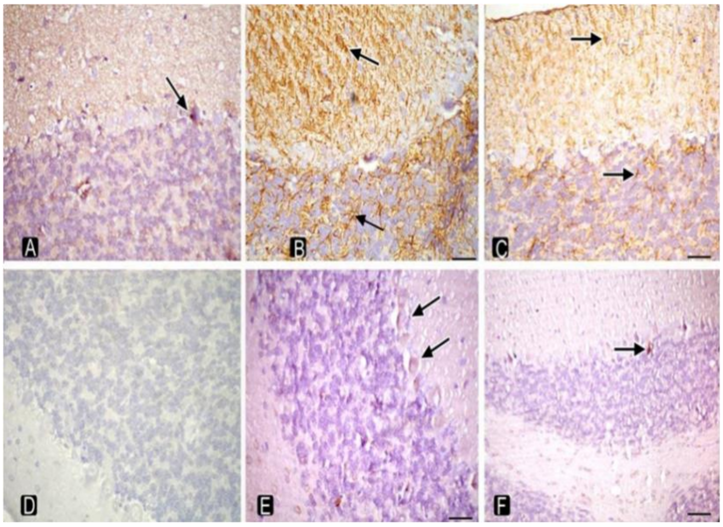

Fig. 2 A, B, C Immunohistochemical GFAP stained sections of cerebellar cortex of albine rat of all studied groups. **A**: control group shows scattered GFAP positive cells in the molecular and granular layers (arrows). **B**: HC group shows abundant large GFAP positive cells (arrows) mainly in the molecular layer and granular layer. **C**: HC – Q 10 group shows few GFAP positive cells (arrows) in the molecular and granular layers. D, E, F: Immunohistochemical Tau stained sections of cerebellar cortex of albine rat of all studied groups. **D:** control group shows negative Tau reaction in all layers of the cerebellar cortex. E: HC group shows Tau positive reaction in the Purkinje cells (arrows). **F:** HC – Q 10 group shows few Tau positive reaction in the Purkinje cells (arrow). (Scale bar=50μm).

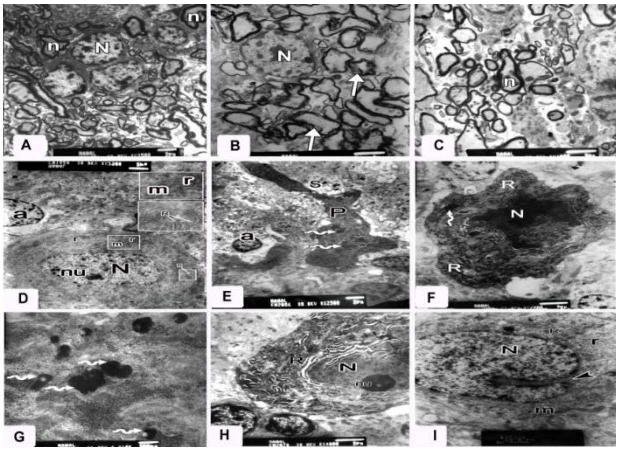

Fig. 3 Electron micrograph of the molecular layer from cerebellar cortex of albino rat of all studied groups. **A:** control group shows cells molecular layer with euchromatic nuclei (N). Almost all nerve fibers (n) are surrounded by normal myelin sheath. X2500 **B:** HC group shows cells molecular layer with euchromatic nuclei (N) with peripheral clumps of heterochromatin. Some nerve fibers have focal areas of myelin sheath separation (arrows). X 4000 **C:** HC–Q 10 group shows cells molecular layer with euchromatic nuclei (N) and nerve fibers (n) having normal myelin sheath. X4000. **D:** shows a Purkinje cell from control rat with euchromatic nucleus (N) and prominent nucleolus. The cytoplasm is rich in small electron dense mitochondria (m), free ribosomes (r) and rough endoplasmic reticulum (R). Bergmann astrocytes (a) with euchromatic nucleus is seen. X2500, both inset. X 10000. D-G show a Purkinje cells of HCD rat with atrophic changes. **E**: shows shrinkage in a Purkinje cell (P) leaving empty spaces (s) around it. Its cytoplasm contains multiple lysosomes (wavy arrows). A Bergmann astrocyte (a) is seen. X2500. **F**: showing; Purkinje cell with ill- defined muddy nucleus and marked indentation of the nuclear membrane (N), dilated rough endoplasmic reticulum (R) and multiple lysosomes (wavy arrow). X4000. **G**: shows multiple lysosomes (wavy arrows) in the cytoplasm of Purkinje cell. X10000. **H**: showing; a Purkinje cell with a euchromatic nucleus (N) and well-defined nucleolus (nu), dilated perinuclear and rough endoplasmic reticulum (R). X4000. **I**: shows Purkinje cell of HC- Q 10 rat having euchromatic nucleus (N) with deep indented nuclear envelop (arrow head), mitochondria (m), ribosomes (r) and short strands of rough endoplasmic reticulum (R). X 6000.

Electron microscopic examination of granular layer from control group, revealed that granule cells had rounded euchromatic nuclei with peripheral clumps of heterochromatin surrounded by a shell of cytoplasm (Fig. 4A). Examination of granular layer from HC group revealed many glial cells with irregular heterochromatic nuclei and thin rim of dark cytoplasm, most probaply oligodendrocytes among the granular cells (Figs 4B&C). Many granule cells had small shrinked heterochromatic pyknotic nuclei (Figs 4B- D). Some granule cell had numerous vacuole like structures. Many astrocyte cells were present among granule cells(Fig. 4E). Granular layer from HC- Q10 group revealed that almost all granule cells had euchromac nuclei with peripheral clumps of heterochromatin and surrounded by a shell of cytoplasm. The cells had small pyknotic heterochromatic nucleus (Fig. 4F).

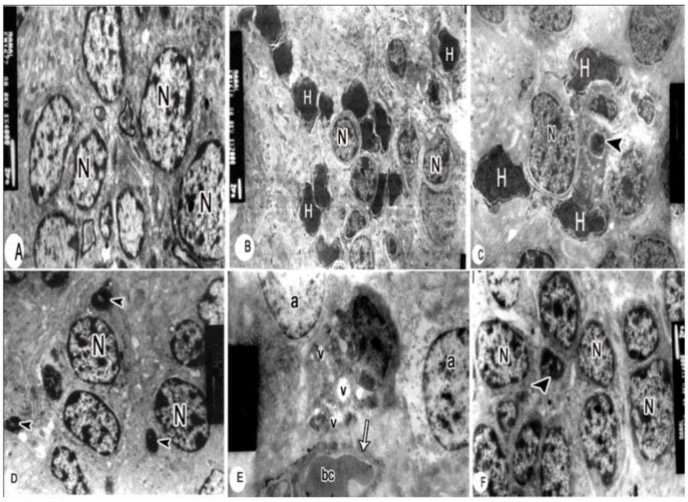

Fig. 4 Electron micrograph of granular layer from cerebellar cortex of albine rat of all studied groups. **A:** shows granule cells from control rat with their rounded euchromatic nuclei (N) with peripheral clumps of heterochromatin surrounded by a shell of cytoplasm. X4000. (B-E) show granular layer of the HC rat. **B**: shows many glial cells with irregular heterochromatic nuclei (H) surrounded by thin rim of dark cytoplasm. Some granule cells have euchromatic nuclei (N). X 2000. **C**: shows small heterochromatic pyknotic cell (arrow head). Some glial cells with irregular heterochromatic nuclei (H) and thin rim of dark cytoplasm are present among the granular cells (N). X 4000. **D**: shows many granule cells' nuclei are small shrinked heterochromatic (arrow heads). Some granule cells appears normal with euchromatic nuclei (N). X4000. **E**: shows a granule cell with numerous vacuole like structures (v). Many astrocyte cells (a) and a blood capillary (bc) with a thick basement membrane (arrow) are seen. X6500 **F**: all granule cells have euchromac nuclei (N) with peripheral clumps of heterochromatin and surrounded by a shell of cytoplasm. One cell with small pyknotic heterochromatic nucleus (arrow head) is seen. X4000.

Electron microscopic examination of blood capillary of the control goup had circular lumen, intact endothelial cell and smooth capillary wall (Fig.5A). HC group revealed that endothelial cells had amorphous nuclear chromatin with epithelial cell protrusions (Fig.5B). Capillary wall degeneration and thickened basal laminae were noticed in most of blood capillaries, expanded perivascular space (Fig.5C) and many collagen fibers around the blood capillaries (Fig. 5D). Blood capillary of the HC – Q 10 group had wide lumen, intact endothelial cell and smooth capillary wall (Fig. 5E).

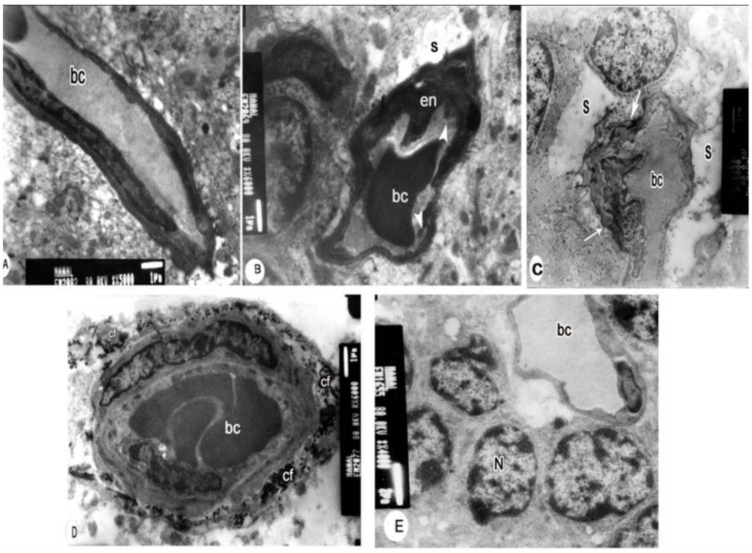

Fig. 5 Electron micrograph of blood capillaries from cerebellar cortex of albine rat of all studied groups. **A:** shows blood capillary (bc) of the control rat with circular lumen, intact endothelial cell and smooth capillary wall. (B-E) show blood capillaries (bc) of the HC rat. **B:** shows that the endothelial cell nuclear chromatin (en) appeare amorphous with epithelial cell protrusions(arrow head). X 6000. **C:** shows expanded perivascular space (s), capillary wall degeneration and thickened basal laminae (arrows). X 5000. **D:** shows many collagen fibers (cf) deposition around the blood capillary (bc). X 6000. **E:** showing; blood capillary (bc) of the HC– Q 10 rat with wide lumen, intact endothelial cell (en) and smooth capillary wall**.** X4000

3.2. Morphometric results

A stereologic analysis showed that the mean total number of Purkinje cells was statistically significant decreased in the rats of HC group (2.25 ±0.34) than in the control animals (4.69 ± 0.17). In HC- Q_{10} group, the number of Purkinje cells was increased up to 3.35 ± 0.08. Cerebellar cortex of HC group showed non significant reduction in the mean values of the thickness of the molecular layer when compared with control group, while there was significant reduction in the thickness of the granule cell layer in comparison with the control group. In HC- Q_{10} group, the granular layer thickness from the HC- Q_{10} group showed a significant increase in comparison with HC group (Table 1).

Table 1 : Mean values of the thickness of the molecular layer (ML) and the granule cell layer (GL) in cerebellar cortex in the different studied groups.

	Group I (Control)	Group II (Q)	Group III (HC)	Group IV (HC-Q10)
ML thickness	84.7± 3.29	80.35±2.27 ^{n}	79.9±2.28 ^{n}	82± 3.42 ^{n}
GL thickness	69.1±2. 50	70.3 ±1.35 ^{n}	32.5 ± 1.85 ^{a}	63.45 ± 0.57 $^{b\,n}$

^{n} non significant difference (P>0.05) comparing to the group I
^{a} significant difference comparing to the group I
^{b} significant difference comparing to the group II

The mean total number of area percentage of GFAP and Tau protein immunoreactivity in cerebellar cortex in the HC group was respectivelly, highly significant and significantly increased comparing to the control group. In HC- Q_{10} group the area percentage of both GFAP and Tau protein reduced become non significant in comparison with the control group (Table 2).

Table 2 : Mean values of the area percentage of GFAP and Tau protein immunoreactivityin cerebellar cortex in the different studied groups.

	Group I (Control)	Group II (Q)	Group III (HC)	Group IV (HC-Q10)
GFAP immunoreactivity area %	3.31 ± 0.48	4.12 ± 0. 43 n	22.17 ± 4.14 ^{b}	5.01±0.23 ^{n}
Tau protein immunoreactivity area %	0.46 ± 0.03	0.52± 0.01 n	5.12± 0.89 ^{a}	0.90± 0.01 ^{n}

^{n} non significant difference (P>0.05) comparing to the group I
^{a} significant difference comparing to the group I
^{b} highly significant difference comparing to the group I

3.3. Biochemical results

HC group showed a significant increase in serum level of both triglycerides, LDL-C and total cholesterol also showed a highly significant increase in comparison to control group, while, HDL-C level was significantly decreased in comparison with the control group. In group HC-Q_{10} the serum level of triglycerides, LDL-C and total cholesterol showed a significant decrease, while HDL-C level was significantly increased in comparison with the HC group (Table 3).

Table 3 : Mean values of serum triglycerides, cholesterol, HDL-C, LDL-C and VLDL-C in the different studied groups expressed as mg/dl.

	Group I (Control)	Group II (Q)	Group III (HC)	Group IV (HC-Q_{10})
Triglycerides	93.89 ± 37.69	104.92±4.34 ^{n}	159.5±6.23 ^{a}	94.67±4.63 $^{c\,n}$
Total cholesterol	105.93 ± 10.66	112.24±5.36	204.30 ±31.79 ^{b}	98.1±4.29 $^{d\,n}$
HDL-C	39.01 ± 3.78	43.52±3.89 ^{n}	24.37±2.80 ^{a}	37.04±3.12 $^{c\,n}$
LDL-C	38.04 ± 13.64	42.32±2.93^{n}	83.91±3.89 ^{b}	40.04±3.72 $^{c\,n}$

^{n} non significant difference (P>0.05) comparing to the group I
^{a} significant difference comparing to the group I
^{b} highly significant difference comparing to the group I
^{c} significant difference comparing to the group III
^{d} highly significant difference comparing to the group III

HC- group showed a significant reduction in all antioxidant markers; SOD, CAT, GPx and a significant increase in oxidative marker MDA in comparison with the control group. HC-Q_{10} group showed significant increase in the SOD, CAT, GPx while, the level of MDA showed significant decrease when compared with the HC group (Table 4).

Table 4 : Mean values of tissue SOD , CAT, GPx and MDA in the different studied groups.

	Group I (Control)	Group II (Q)	Group III (HC)	Group IV (HC-Q_{10})
SOD	12.2 ± 0.90	13.5 ± 0.99 ^{n}	9.2 ± 0.75	13.0 ± 0.96
CAT	23.0 ± 1.70	24.31 ±0.21	17.5 ± 1.45	26.0 ± 2.02
GPx	9.90 ± 0.73	10.30 ± 0.76 ^{n}	6.76±1.43	10.40 ± 0.77
MDA	0.85 ± 0.06	0.91 ± 0.07^{n}	1.65 ± 0.07	0.79 ± 0.05

^{n} non significant difference (P>0.05) comparing to the group I
^{a} significant difference comparing to the group I
^{b} highly significant difference comparing to the group I
^{c} significant difference comparing to the group III

IV. Discussion

Serum cholesterol has been suggested as a risk factor or modulator of neurological diseases although the effects appear complex and disease specific [15]. In the present study, increases of body weight were detected in high cholesterol group compared with control value. Similar observations were reported in several studies [26 & 27].

The current study showed shrinkage in a Purkinje cells leaving empty spaces around them. Its cytoplasm contains multiple lysosomes, dilated perinuclear and rough endoplasmic reticulum cisternae. Many Purkinje cells had ill defined muddy nuclei. Cerebellar cells grown in cell culture with cholesterol produced neurodegeneration as indicated by altered morphology, less synaptic connections, and cell shrinkage as compared to normal cells [28]. Cholesterol-enriched diet caused intracellular lipid accumulation and several alterations in the structural and functional properties of the other organs as myocardium [29]. The numerous dense bodies were degenerating mitochondria. The dense bodies contained acid phosphatase, and considered as lysosomes [30]. Autophagocytosis followed by lysosomal processing is the major degradative pathway for mitochondria, a process sometimes abbreviated as "mitophagy" [31] which would account for the transitional forms between normal mitochondria and the lamellar bodies in dystrophic neurites of amyloid plaques [30]. Excessicve cholesterol can participate in alzaheimer disease [28].

In the current study, the significant decrease in the number of Purkinje cells was correlated with the decreased volume of the granular and molecular layers. Purkinje cell density is decreased, in neurodegenerative diseases as AD [32].

In the current study some apoptotic granular cells were detected. Excessive cholesterol leads to apoptosis and cell death [28]. Apoptosis has been implicated in the pathogenesis of various neurodegenerative diseases like AD [33 & 34]. Hypercholesterolemia, activate mitochondrial-dependent apoptotic pathway. The decreasaed Bcl-2, and increased cytochrome c release, increased activated-caspase 9 and increased caspase 3 were detected in the heart of hypercholesterolemia hamaster [35] . Long term high cholesterol diet induced increase the expression of the proinflammatory cytokine interleukin- 6 and of caspase-1 in the brain [36].

The present study revealed that blood vessels from cerebellar cortex of rats from HC group had variable degree of affections. Some vessels had nuclei with amorphous chromatin, epithelial cell protrusions, capillary wall degeneration and thickened basal laminae. Collagen fibers deposition around the blood capillaries and expanded perivascular space were seen. This pathology is distinctive from cholesterol-induced atherosclerotic disease but shares some features of the microvascular pathology associated with a variety of neurological diseases like AD, as the thickened basement membranes [37].

Previous researches have shown that high cholesterol diets induce microvascular dysfunction [38 & 39]. High dietary cholesterol have been implicated in increase vascular permeability and associated with some neurological disorders (especially stroke and Alzheimer's disease) [40]. Expanded perivascular space and perivascular swelling is similar to those observed in diabetic rats and could represent swollen pericytes, astrocytes, or adipocytes leading to disruption of the blood brain barrier (BBB) functions [41]. The generation of reactive oxygen species, in particular superoxide is thought to be a major factor in cholesterol's effects on dysfunction of the microvasculature [42].

Significant upregulation GFAP immunohistochemical expression has been demonstrated in HC goup. Microglial activation, astrocytosis were the major immunohistochemical features observed in the brain of rabbit fed with high cholsterol diet [43]. Although activated astrocytes secrete different neurotrophic factors for neuronal survival [44], marked astrocyte activation evidenced by increased GFAP expression has been associated with the release of inflammatory cytokines, reactive oxygen species and an alteration in the extracellular space [45]. Astrocytosis could be explained by the fact that excessive cholesterol can produce rigidity and loss of membrane fluidity in neurons and formation of cell debris. The formed debris can act as antigen and trigger inflammatory response and/or gliosis [28]. The astrocytes repair damage by filling spaces left by the degeneration of parts of nerve fibers and neurons and phagocytose some degenerating myelin. Amyloid plaques, a pathologic hallmark of AD, are associated with GFAP positive activated astrocytes [46]. Astrocytes and Microglia and may be consumers of amyloid plaques rather than producers [47].

The current study showed Tau positive reaction in the many Purkinje cells of HC group. These results were in consistent with previous investigators who have shown that cholesterol-enriched diets induce hyperphosphorylation of tau, and neuronal cell death [40].

Numerous studies suggested cytotoxic effects of metabolite of cholesterol like oxysterols are associated with neurodegenerative diseases [48]. Cholesterol may efficiently cross the BBB after undergoing specific hydroxylation at the 27 and 24 positions by 27-hydroxylase enzyme and 24-hydroxylase which being located exclusively in CNS, respectively [49 & 50]. Cholesterol metabolites such as Oxysterols, synthesized in the periphery would find it much easier to reach the brain than cholesterol itself [51]. Another possibility is that the high-cholesterol diet may affect the ratio of esterified to non-esterified cholesterol in the brain. Cholesterol esterification has been implicated in the production of β-amyloid, the toxic peptide associated with AD [52]. The molecular mechanisms involved in the pathogenesis of high cholesterol diet effects on the cerebellum need further investigation. Previous researches clarify that long term high cholesterol diet induced mild changes the gene expression in the mouse brain. Some of the altered genes were earlier shown to be involved in neurodegenerative disorderes especially in AD [46].

In the current work, light microscope examination of sections of the cerebellum of rats from HC- Q $_{10}$ group showed that they resumed nearly their normal general architecture except for few Tau positive reaction in the Purkinje cells. Co Q_{10} acts as an electron carrier in the mitochondrial respiratory chain and it is an essential cofactor of the electron transport gene. It has been demonstrated that CoQ $_{10}$ can protect against lesions produced by the mitochondrial toxins. CoQ $_{10}$ can significantly extend survival, delay motor deficits and delay weight loss and attenuate the development of striatal atrophy in a transgenic mouse model of HD [53]. It is involved in the reactive oxygen species removal and prevention of oxidative stress-induced apoptosis. In addition, it has potential benefits to decrease inflammation and to enhance neuroprotection [54]. Co Q_{10} dramatically reduced apoptotic cell death [55]. As a result, oral absorption of lipophilic Co Q_{10} is frequently slow, and its variable bioavailability depends on the presence of postprandial lipids in the gastrointestinal tract. Body weight was nearly that of the control group. Co Q_{10} decreased storage of fat as well as protein [56].

The present blood biochemical study demonstrated that high cholesterol diet in rats caused a significant increase in serum level of both triglycerides and LDL-C while, total cholesterol showed a highly significant increase in comparison to control group, while, HDL-C level was significantly decreased in comparison with the control group. In group HC-Q_{10} the serum level of triglycerides, LDL-C and total cholesterol showed a significant decrease, while HDL-C level was significantly increased in comparison with the HC group. Singh et al. reported that Co Q_{10} reduce the lipid levels and increase in HDL-C levels due to inhibition of LDL-C oxidation and reduce oxidative stress [57]. Moreover, Modi et al. stated that the Co Q_{10} lowered serum triglycerides due to either a decrease in VLDL-C synthesis or channeling of VLDL-C to pathway other than to LDL or an increase in lipoprotein lipase activity [58]. In addition, higher total serum cholesterol and LDL-C correlate with a more rapid cognitive decline in patients with AD [59].

The treatment of animals feeding high cholesterol diet, with Co Q_{10} reduced lipid concentration in liver mitochondria with no effect on plasma lipids, increased mitochondrial levels of alpha-tocopherol, restored mitochondrial Co Q_{10} and improved alpha-tocopherol levels in plasma. The present reduction in the values of lipid profile levels may be due to inhibition of hepatic cholesterol synthesis, or the redistribution of cholesterol from plasma to the liver by the cholesterol-metabolizing enzyme systems in the liver or the control of lipids utilization [60].

The present tissue biochemical study shoewd that feeding with a high cholesterol diet caused a significant reduction in all antioxidant markers; SOD, CAT, GPx and a significant increase in oxidative marker MDA in comparison with the control group. Coenzyme-Q $_{10}$ supplementation made a significant increase in the antioxidant markers while, the level of oxidative marker MDA showed significant decrease comparing with the HC group. These results were in accordance with previous researches [58]. The relationship between oxidative stress and cholesterol levels was confirmed in many studies [61 - 63]. Basco and coworkers have demonstrated that cholesterol metabolites are cytotoxic and play role in generation of reactive oxygen species(ROS) [64].

V. Conclusion

Together , the structural and biochemical data of this study indicated that high cholesterol diet has a deletorious effect on the histological and biochemical structure of cerebellar cortex. There is a possible role of oxidative stress in the present results showed that Co Q_{10} ameliorates these effects. Nutritional awareness for cholesterol ratio in diet is critical and antioxidant co enzyme Q_{10} is recommended as a neuroprotective agent for at risk population.

VI. Conflict Of Interest

No conflict of interest

References

[1]. Ghez C, Fahn S (1985) The cerebellum, in Principles of Neural Science, 2nd edition, edited by Kandel ER, Schwartz JH. New York, Elsevier, pp 502–522

[2]. Ito M. (2008) Control of mental activities by internal models in the cerebellum. Nat Rev Neurosci;9:304–313.

[3]. Adibhatla RM, Hatcher JF. (2007) Role of Lipids in Brain Injury and Diseases. Future Lipidol. Aug;2(4):403-422.

[4]. Rubinstein J, Pelosi A, Vedre A, Pavan Kotaru P and George S Abela(2009) Hypercholesterolemia and Myocardial function evaluated via Tissue Doppler Imaging. Cardiovascular Ultrasound, 7:56.

[5]. Kirsch C, Eckert GP, Koudinov AR, Müller WE. (2003) Brain cholesterol, statins and Alzheimer's Disease. Pharmacopsychiatry. Sep;36 Suppl 2:S113-119.

[6]. Gosselet F (2011) The Mysterious Link between Cholesterol and Alzheimer's Disease: Is the Blood-Brain Barrier a Suspect? Gosselet J Alzheimers Dis Res, Volume 1 Issue 1.

[7]. Dehouck B, Fenart L, Dehouck MP, Pierce A, Torpier G, Cecchelli R. (1997) A new function for the LDL receptor: transcytosis of LDL across the blood-brain barrier. J Cell Biol. Aug 25;138(4):877-89.

[8]. Sparks, D.L. and Schreurs, B.G. (2003) Trace amounts of copper in water induce β-amyloid plaques and learning deficits in a rabbit model of Alzheimer's disease. Proc. Natl. Acad. Sci. U.S.A. 100, 11065–11069 .

[9]. Simon KC, Chen H, Schwarzschild M, Ascherio A (2007) Hypertension, hypercholesterolemia, diabetes, and risk of Parkinson disease. Neurology , 69(17):1688-1695.

[10]. Sharma M, Ansari MT, Abou-setta AM, Soares-Weiser K, Ooi TC, Sears M, et al. (2009) Systematic Review: Comparative Effectiveness and Harms of Combinations of Lipid-Modifying Agents and High-Dose Statin Monotherapy. Ann. Int. Med.;151.
[11]. Stamer K, Vogel R, Thies E, Mandelkow E and Mandelkow EM. (2002): Tau blocks traffic of organelles, neurofilaments and APP vesicles in neurons and enhances oxidative stress. J.Cell Biol. Mar 18;156(6):1051-1063.
[12]. Dickey C, Kraft C, Jinwal U, Koren J, Johnson A anderson L, Lebson L, Lee D, Dickson D, de Silva R, Binder LI, Morgan D and Lewis J. (2009): Molecular pathogenesis of genetic and inherited diseases aging analysis reveals slowed tau turnover and enhanced stress response in a mouse model of tauopathy. Am.J.Pathol. Jan;174(1):1-11.
[13]. Rosenfeldt, F. D. Hilton, S. Pepe and H. Krum, (2003) Systematic review of effect of coenzyme Q10 in physical exercise, hypertension and heart failure. Biofactors, 18: 91-100. PMID: 14695924.
[14]. Spindler, M. M.F. Beal and C. Henchcliffe, (2009) Coenzyme Q10 effects in neurodegenerative disease. Neuropsychiatr Dis. Treat. 5: 597-610. PMID: 19966907
[15]. Franciosi S , Sosa MAG , English DF, Oler E, Oung T, Janssen W GM, Gasperi RD, Schmeidler J , Dickstein DL , Schmitz C, Gandy S , Hof PR , Buxbaum JD and A Elder G. Novel cerebrovascular pathology in mice fed a high cholesterol diet. Novel cerebrovascular pathology in mice fed a high cholesterol diet.
[16]. Ramos-Vara JA, Kiupel M, Baszier T, Bliven L, Brodersen B, Chelack B, et al. (2008) Suggested guidelines for immunohistochemical techniques in veterinary diagnostic laboratories. J Vet Diagn Invest; 20:393–413.
[17]. Glauert AM, Lewis PR. (1998) Biological specimen preparation for transmission electron microscopy. 1st ed. London: Portland Press.
[18]. Bancroft JD, Gamble M. (2008) Theory and practice of histological techniques. 6th ed. Philadelphia, PA: Churchill Livingstone.
[19]. Axelrad JE, Louis ED, Honig LS, Flores I, Ross GW, Pahwa R, et al.(2008) Reduced Purkinje cell number in essential tremor: a postmortem study. Arch Neurol; 65:101–107.
[20]. Stein E.A. and G. L. Myers (1995) "National cholesterol education program recommendations for triglyceride measurement: executive summary," Clinical Chemistry, vol. 41, no. 10, pp. 1421–1426
[21]. Braun H. P. (1984)"National cholesterol education programme. Recommendations for cholesterol measurements," Chemistry, vol. 30, pp. 991–199.
[22]. Kono Y. (1978) Generation of superoxide radical during autoxidation of hydroxylamine and an assay for superoxide dismutase. Arch Biochem Biophys; 186:189–195.
[23]. Aebi H. Catalase in vitro. Methods Enzymol (1984); 105:121–126.
[24]. Flohe L, Gunzler WA. (1984) Assays of glutathione peroxidase. Methods Enzymol; 105:114–121.
[25]. Drury, R. A. B. and Wallington, E. A. (1980): Carleton's histological techniques. 5th ed. London: Oxford University Press.
[26]. Amin, K.A. and M.A. Nagy, (2009) Effect of Carnitine and herbal mixture extract on obesity induced by high fat diet in rats. Diabetol. Metab. Syndr. 1: 17.
[27]. Koya-Miyata, S. N. Arai, A. Mizote, Y. Taniquchi and S. Ushio et al. 2009. Propolis prevents dietinduced hyperlipidemia and mitigates weight gain in diet-induced obesity in mice. Biol. Pharm. Bull. 32: 2022-2028.
[28]. Ramanathan M and Deshmuk D. (2009) Effect of excessive cholesterol amnd lipopolysacharide on cerebellar neuronal cells in in vitro and prtotectivre role of anti-inflammatory drugs.. Indian journal of experimental biology. 47: 320-326.
[29]. Puskas LG, Nagy ZB, Giricz Z, Onody A, Csonka C, Kitajka K, et al. (2004) Cholesterol diet-induced hyperlipidemia influences gene expression pattern of rat hearts: a DNA microarray study. FEBS Lett;562:99–104.
[30]. Fiala CJ. (2007) Mechanisms of amyloid plaque pathogenesis. Acta Neuropathol 114:551–571.
[31]. Brunk UT, Terman A (2002) The mitochondrial–lysosomal axis theory of aging: accumulation of damaged mitochondria as a result of imperfect autophagocytosis. Eur J Biochem 269:1996–2002.
[32]. Fukutani Y, Cairns NJ, Rossor MN, et al (1996) Purkinje cell loss and astrocytosis in the cerebellum in familial and sporadic Alzheimer's disease. Neurosci Lett; 214:33–36
[33]. Yuan G. J.; Yankner, B.A. (2000) Apoptosis in the nervous system. Nature, 407, 802–809.
[34]. Zarow C, Barron E, Chui HC, Perlmutter LS(1997) Vascular basement membrane pathology and Alzheimer's disease. Ann N Y Acad Sci, 826:147-160.
[35]. Bertoni-Freddari, C.; Fattoretti, P.; Casoli, T.; di Stefano, G.; Balietti, M.; Giorgetti, B; Perretta (2009) Neuronal apoptosis in Alzheimer's disease: The role of age-related mitochondrial metabolic competence. Ann. N. Y. Acad. Sci, 1171, 18–24.
[36]. Kuo WW, Hsu TC, Chain MH, Lai CH, Wang WH, Tsai FJ, Tsai CH, Wu CH, Huang CY, and Tzang BS. (2011) Attenuated CardiacMitochondrial-Dependent Apoptotic Effects by Li-Fu Formula in Hamsters Fed with a Hypercholesterol Diet. Evidence-Based Complementary and Alternative Medicine; Article ID 530345, 9 pages doi:10.1093/ecam/nep182.
[37]. Rahman SMA. (2006) Thesis , Studies on Apolipoprotein and High Cholesterol Diets as Risk Factors for Neurodegeneration. Karolinska Institutet stockholm, Larserics Digital Print AB Stockholm Sweden.
[38]. Bailey TL, Rivara CB, Rocher AB, Hof PR (2004): The nature and effects of cortical microvascular pathology in aging and Alzheimer's disease. Neurol Res, 26(5):573-578.
[39]. 38-VanTeeffelen JW, Constantinescu AA, Vink H, Spaan JA (2005) Hypercholesterolemia impairs reactive hyperemic vasodilation of 2A but not 3A arterioles in mouse cremaster muscle. Am J Physiol Heart Circ Physiol, 289(1):H447-454.
[40]. 39-Ellis A, Cheng ZJ, Li Y, Jiang YF, Yang J, Pannirselvam M, Ding H, Hollenberg MD, Triggle CR (2008) Effects of a Western diet versus high glucose on endothelium-dependent relaxation in murine micro- and macro-vasculature. Eur J Pharmacol, 601(1-3):111-117.
[41]. Ghribi O, Golovko MY, Larsen B, Schrag M, Murphy EJ (2006) Deposition of iron and beta-amyloid plaques is associated with cortical cellular damage in rabbits fed with long-term cholesterolenriched diets. J Neurochem, 99(2):438-449.
[42]. Hern´andez-Fonseca JP. Rinc ´ on J. Pedrea˜nez A. Viera N, Arcaya JL, Carrizo E, and Mosquera J. (2009) Structural and Ultrastructural Analysis of Cerebral Cortex, Cerebellum, and Hypothalamus from Diabetic Rats. Experimental Diabetes Research Volume, Article ID 329632, 12 pages doi:10.1155/2009/329632.
[43]. Stokes KY (2006) Microvascular responses to hypercholesterolemia: the interactions between innate and adaptive immune responses. Antioxid Redox Signal, 8(7-8):1141-1151.
[44]. 42-Thirumangalakudi L, Prakasam A, Zhang R, Bimonte-Nelson H, Sambamurti K, Kindy MS, Bhat NR (2008) High cholesterol-induced neuroinflammation and amyloid precursor protein processing correlate with loss of working memory in mice. J Neurochem, 106(1):475-485.
[45]. Williams A, Piaton G, Lubetzki C (2007) Astrocytes–friends or foes in multiple sclerosis. Glia 55(13):1300–1312
[46]. Groebe A. & Clarner T. & Baumgartner W. & Dang J. & Beyer C. & Kipp M (2009) Cuprizone Treatment Induces Distinct Demyelination, Astrocytosis, and Microglia Cell Invasion or Proliferation in the Mouse Cerebellum. Cerebellum 8:163–174.

[47]. Peters A. (2007) The Effects of Normal Aging on Nerve Fibers and Neuroglia in the Central Nervous System. In: Riddle DR, editor. Brain Aging: Models, Methods, and Mechanisms. Boca Raton (FL): CRC Press; Chapter 5. Frontiers in Neuroscience.

[48]. 48-Wyss-Coray T, Loike JD, Brionne TC, Lu E, Anankov R, Yan F, Silverstein SC, Husemann J (2003) Adult mouse astrocytes degrade amyloid-beta in vitro and in situ. Nat Med 9:453–457.

[49]. Manukhina, E. B. F. Wiegant, V. I. Torshin, A. V. Goryacheva, I. P. Khomenko, S. V. Kruglov, S. Yu. Mashina, D. A. Pokidyshev, E. A. Popkova, M. G. Pshennikova, M. A. Vlasova, O. M. Zelenina, and I. Yu. Malyshev (2004) Prospects of Non-drug Approaches to Alzheimer's Disease. Biology Bulletin, Vol. 31, No. 4, pp. 382–395.

[50]. Bjorkhem I, Cedazo-Minguez A, Leoni V, Meaney S (2009) Oxysterols and neurodegenerative diseases. Mol Aspects Med 30: 171-179.

[51]. Jeitner TM, VoloshynaI, Reiss AB (2011) Oxysterol derivatives of cholesterol in neurodegenerative disorders. Curr Med Chem 18: 1515-1525.

[52]. Björkhem I. (2002) Do oxysterols control cholesterol homeostasis? J Clin Invest. Sep;110(6):725-730.

[53]. Puglielli L, Konopka G, Pack-Chung E, Ingano LA, Berezovska O, Hyman BT, Chang TY, Tanzi RE, Kovacs DM. Acyl-coenzyme A (2001) cholesterol acyltransferase modulates the generation of the amyloid beta-peptide. Nat Cell Biol. Oct;3(10):905-12.

[54]. Beal, MF (2002). Coenzyme Q 10 as a Possible Treatment for Neurodegenerative Diseases. Free Radical Research, 2002, Vol. 36, No. 4, Pages 455-460.

[55]. Kunitomo M, Yamaguchi Y, Kagota S, Otsubo K. (2008) Beneficial effect of coenzyme Q10 on increased oxidative and nitrative stress and inflammation and individual metabolic components developing in a rat model of metabolic syndrome. J Pharmacol Sci; 107:128–137.

[56]. Kernt M, Hirneiss C, Neubauer AS, Ulbig MW, Kampik A. (2010) Coenzyme Q10 prevents human lens epithelial cells from light-induced apoptotic cell death by reducing oxidative stress and stabilizing BAX/Bcl-2 ratio. Acta Ophthalmol; 88:e78–e86.

[57]. -Attar A M.. (2010) Hypolipidemic Effects of Coenzyme Q10 in Experimentally Induced Hypercholesterolemic Model in Female Rats. American Journal of Pharmacology and Toxicology 5 (1): 14-23.

[58]. Singh, R.B. S.N. Shinde, R.K. Chopra, M.A. Naiz and A.S. Thakur et al. (2000). Effect of coenzyme Q10 on experimental atherosclerosis and chemical composition and quality of atheroma in rabbits. Atherosclerosis, 148: 275-282.

[59]. Modi, K. D.D. Santani, R.K. Goyal and P.A. Bhatt, (2006) Effect of coenzyme Q10 on catalase activity and other antioxidant parameters in streptozotocin-induced diabetic rats. Biol. Trace Elem. Res. 109: 25-34.

[60]. Helzner EP, Luchsinger JA, Scarmeas N, Cosentino S, Brickman AM, Glymour MM, Stern Y (2009) Contribution of vascular risk factors to the progression in Alzheimer disease. Arch Neurol , 66(3):343-348.

[61]. Ramirez-Tortosa, M.C. S. Granados, C.L. Ramirez- Tortosa, J.J. Ochoa and P. Camacho et al. (2008) Oxidative stress status in liver mitochondria and lymphocyte DNA damage of atherosclerotic rabbits supplemented with water soluble coenzyme Q10. Biofactors, 32: 253-273.

[62]. Balkan, J. S.D. Ru-Abbasoglu, G. Aykac-Toker and M. Uysal, (2004) The effect of a high cholesterol diet on lipids and oxidative stress in plasma, liver and aorta of rabbits and rats. Nutr. Res. 24: 229-234.

[63]. Chang, W.C. Y.M. Yu, Y.M. Hsu, C.H. Wu and P.L. Yin et al. (2006) Inhibitory effect of Magnolia officinalis and lovastatin on aortic oxidative stress and apoptosis in hyperlipidemic rabbits. J. Cardiovasc. Pharmacol. 47: 463-468.

[64]. Codoñer-Franch, P. A.B. López-Jaén, P. Muñiz, E. Sentandren and V.V. Bellés, (2008) Mandarin juice improves the antioxidant status of hypercholesterolemic children. J. Pediatr. Gastroenterol. Nutr. 47: 349-355.

[65]. Bosco DA, Fowler DM, Zhang Q, Nieva J, Power ET, Wentworth Pjr, Lemer RA and Kelly JW. (2006) Elevated levels of oxidized cholesterol metabolites in Lewy body disease brains accelerate alpha-synuclein fibrilization, Nat Chem Biol, 2: 249.